AIP | Applied Physics Letters

InGaAs/GaP quantum dot light-emitting diodes on Si

Yuncheng Song and Minjoo Larry Lee

Citation: Appl. Phys. Lett. **103**, 141906 (2013); doi: 10.1063/1.4824029
View online: http://dx.doi.org/10.1063/1.4824029
View Table of Contents: http://apl.aip.org/resource/1/APPLAB/v103/i14
Published by the AIP Publishing LLC.

InGaAs/GaP quantum dot light-emitting diodes on Si

Yuncheng Song[a] and Minjoo Larry Lee
Department of Electrical Engineering, Yale University, New Haven, Connecticut 06520-8284, USA

(Received 30 August 2013; accepted 16 September 2013; published online 1 October 2013)

We report on the growth, structure, and luminescence of $In_{0.5}Ga_{0.5}As$/GaP self-assembled quantum dots (SAQDs) on exact Si (001) by means of an epitaxial GaP/Si template. *In situ* reflection high-energy electron diffraction showed indistinguishable transitions during SAQD growth, indicating similar growth kinetics on GaP/Si and bulk GaP. $In_{0.5}Ga_{0.5}As$ SAQD stacks on both substrates yielded nearly identical photoluminescence spectra, with peak position, peak-width, and integrated intensity varying by <5%. We then describe the characteristics of $In_{0.5}Ga_{0.5}As$/GaP SAQD light-emitting diodes on Si. These results demonstrate that combining $In_{0.5}Ga_{0.5}As$/GaP SAQDs with GaP/Si templates provides a novel path for monolithic integration of optoelectronics with Si. © *2013 AIP Publishing LLC*. [http://dx.doi.org/10.1063/1.4824029]

The advancement of high-quality GaP on Si (001)[1–6] has enabled a new platform for monolithic integration of III-V optoelectronic devices with Si-based electronics, including Ga(NAsP) quantum well lasers[7] and metamorphic GaAsP solar cells.[8,9] $In_xGa_{1-x}As$ self-assembled quantum dots (SAQDs) grown on GaP offer another path to integration of direct-bandgap material onto indirect GaP/Si templates. Since their initial demonstration via solid-source molecular beam epitaxy (MBE),[10] $In_xGa_{1-x}As$ SAQDs have been grown on GaP by both gas-source MBE[11] and metallorganic chemical vapor deposition,[12] while further study has been devoted to understanding their atomic structure, band structure, and device applications. For example, Prohl *et al.* used cross-sectional scanning tunneling microscopy to show that $In_xGa_{1-x}As$/GaP SAQDs have a truncated pyramidal profile and an indium-rich core, similar to InAs/GaAs SAQDs.[13] Calculations using $\boldsymbol{k}\cdot\boldsymbol{p}$ and tight-binding models were also used to show that $In_xGa_{1-x}As$/GaP SAQDs possess a direct band structure and a type-I band offset for dot diameters >20 nm and In content >30%.[14,15] Furthermore, Rivoire *et al.* studied $In_{0.5}Ga_{0.5}As$ SAQDs embedded within GaP photonic crystals for single QD applications.[16] Recently, we reported on room-temperature electroluminescence (EL) from $In_{0.5}Ga_{0.5}As$ SAQDs grown on bulk GaP, showing their viability for optoelectronic applications.[17] While $In_xGa_{1-x}As$ SAQDs exhibit promising properties on bulk GaP, to date, there have been no studies of similar SAQDs on Si.

In this work, we report the growth of $In_{0.5}Ga_{0.5}As$ SAQDs on exact Si (001) by means of an epitaxial GaP/Si template. A combination of *in situ* reflection high-energy electron diffraction (RHEED) observation, cross-sectional transmission electron microscopy (XTEM), and room-temperature photoluminescence (PL) spectroscopy shows that the SAQDs are nearly identical on both bulk GaP and GaP/Si templates. We also describe the characteristics of $In_{0.5}Ga_{0.5}As$/GaP SAQD light-emitting diodes (LEDs) on Si, showing the feasibility of using $In_{0.5}Ga_{0.5}As$ SAQDs as the active medium in monolithic integration of high-performance light emitters on Si.

Growth was carried out using solid-source MBE on both high-quality epitaxial GaP/Si templates and bulk GaP. GaP/Si templates were provided by $NAsP_{III/V}$ GmbH and consisted of a 1 μm *n*-type Si homoepitaxial buffer followed by a 46 nm *n*-type GaP nucleation layer/cap, all grown on a 300 mm (001) on-axis *p*-type Si substrate. Atomic force microscopy (AFM) on the as-received templates gave a root mean square (RMS) roughness of 0.73 nm over a $10 \times 10\ \mu m^2$ area, confirming that the nucleation procedure[5] yielded a smooth morphology. The pseudomorphic GaP layer is below the critical thickness of 70 nm on Si[5] and possesses minimal anti-phase disorder; the previous work showed that all anti-phase domains are self-annihilated within ~40 nm.[5] To facilitate sample heating and handling in the MBE chamber, GaP/Si template pieces were cleaved from the same 300 mm starting wafer and indium-mounted to 100 mm Si backing wafers prior to growth. No pre-cleaning was performed.

After oxide desorption of the GaP nucleation layer at 650 °C for 30 min under P_2 overpressure, the growth started with a homoepitaxial GaP buffer at 590 °C using a P_2/Ga beam equivalent pressure (BEP) ratio of ~10 and a growth rate of 0.5 μm/h. Temperatures reported here were measured by pyrometer, and BEP ratios were estimated from pressures read directly off of a beam flux monitor at the substrate position. During oxide desorption, the RHEED exhibited a spotty pattern with a low intensity background, similar to what is observed during oxide desorption of bulk GaP. After initiating growth, the RHEED pattern evolved into a streaky (2×4) reconstruction within 15 nm of GaP deposition, indicating smooth, single-domain growth. The (2×4) pattern remained throughout the GaP buffer growth, and a 250 nm GaP buffer on GaP/Si had a 1.99 nm RMS roughness in a $10 \times 10\ \mu m^2$ AFM scan. The lattice mismatch of GaP and Si at the growth temperature is ~0.46%,[18] and misfit dislocations at the GaP/Si interface form as the critical thickness is exceeded. The slight increase in RMS roughness from 0.73 to 1.99 nm is due to the emergence of a cross-hatch pattern on the GaP surface, as expected for a relaxed mismatched layer.[6]

In situ RHEED observation shows that the growth dynamics of $In_{0.5}Ga_{0.5}As$ SAQDs on GaP/Si templates and bulk GaP were identical. SAQD samples were grown on

[a]Electronic mail: yuncheng.song@yale.edu

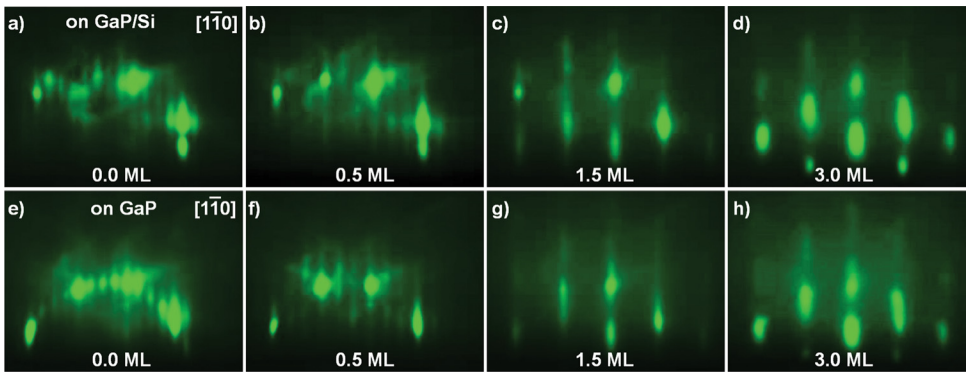

FIG. 1. RHEED evolution during SAQD growth on (a)–(d) GaP/Si template and (e)–(h) bulk GaP. The patterns are extremely similar in both cases.

both types of substrates at 470 °C with a growth rate of 0.16 monolayer (ML) per second and an As_2/(Ga + In) BEP ratio of ~40. Similar to our previous work,[10,17] $In_{0.5}Ga_{0.5}As$ refers to a nominal 50% In composition. After initiating the SAQD growth on a smooth GaP/Si buffer, the [1$\bar{1}$0] azimuth RHEED pattern converted from streaky 4× [Figure 1(a)] to a streaky 3× [Figure 1(b)] at 0.5 ML of $In_{0.5}Ga_{0.5}As$ coverage, indicating the formation of a smooth, reconstructed InGaAs(P) layer. The streaky 3× pattern dissipated with additional $In_{0.5}Ga_{0.5}As$ deposition and the RHEED pattern underwent a transition from streaky to spotty at ~1.5 ML of $In_{0.5}Ga_{0.5}As$ coverage [Figure 1(c)]. SAQD growth was terminated at 3.0 ML deposition, by which point the RHEED had evolved to a bright spotty pattern [Figure 1(d)]. After covering the SAQDs with a 10 nm GaP spacer at 470 °C and annealing at 560 °C for 10 min, the RHEED reverted to a streaky (2 × 4) pattern. A control sample on bulk GaP with the same growth procedures showed a one-to-one correspondence in RHEED patterns [Figures 1(e)–1(h)] when compared with growth on a GaP/Si template. Therefore, we find that $In_{0.5}Ga_{0.5}As$ SAQD growth kinetics on GaP/Si are not affected by the presence of cross-hatch roughness[19] or any residual lattice strain[20] in the GaP. Planar-view TEM images of capped dots (not shown) showed that the growth conditions used here yielded a dot density of $2.7 \times 10^{10}\,cm^{-2}$ and a diameter of 32 ± 6 nm.

XTEM revealed the microstructural similarity and coherent nature of $In_{0.5}Ga_{0.5}As$ SAQDs on both substrates. The low-magnification, $\boldsymbol{g} = 004$ bright-field XTEM image in Figure 2(a), shows a stack of 8 periods of $In_{0.5}Ga_{0.5}As$ SAQDs embedded in the middle of a 650 nm GaP layer grown on a GaP/Si template. No anti-phase disorder, stacking faults, or microtwins are found in the III-V layers, while the dark contrast at the bottom of the GaP buffer results from an array of misfit dislocations formed at the GaP/Si interface. The formation of this misfit array can be avoided by using a Ga(PN) (Ref. 21) or (BGa)P (Ref. 22) buffer to achieve true lattice-matching with the underlying Si substrate. A higher-magnification XTEM image around the SAQD stack shows 8 periods of SAQDs and spacers [Figure 2(b)]. In this image, the presence of 8 wetting layers confirms the Stranski-Krastanov growth mode for every SAQD layer, and the strain contrast around the SAQDs matches that seen in our earlier $In_{0.5}Ga_{0.5}As$/GaP SAQDs.[10] We also performed XTEM on a control sample with the same structure grown under identical conditions on bulk GaP. As shown in Figures 2(b) and 2(c), the SAQD stacks on both substrates have very similar microstructure, which is consistent with the *in situ* RHEED observations.

Room-temperature PL of 8-period SAQD stacks simultaneously co-grown on both substrates exhibit spectra with the same peak wavelengths of 674 nm (1.84 eV) (Figure 3), suggesting that the shape and composition of SAQDs are very similar in both cases. Furthermore, the PL spectra from both substrates differ by <5% in both integrated intensity and full width at half maximum (FWHM), indicating similar internal quantum efficiency and dot size distributions, respectively. With nearly identical characteristics observed in RHEED, XTEM, and room-temperature PL, we conclude

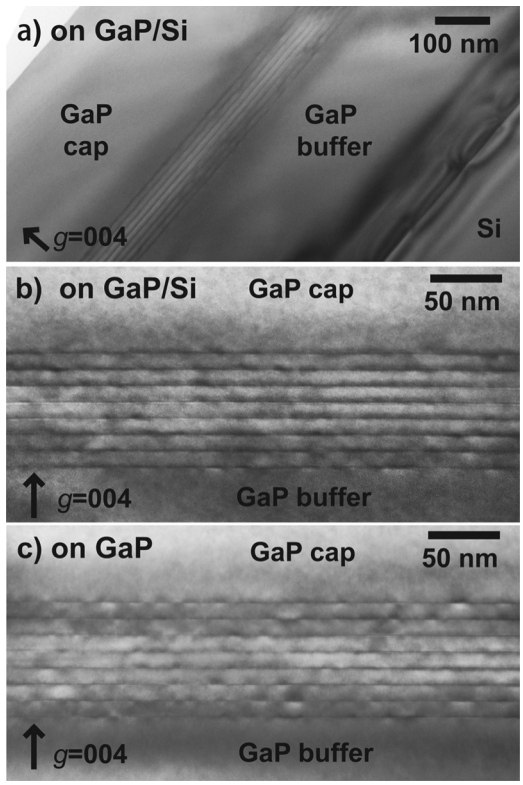

FIG. 2. (a) Low-magnification, $g = 004$ bright field XTEM image showing entire epitaxial structural of an 8-period $In_{0.5}Ga_{0.5}As$ SAQD stack on GaP/Si. No extended defects are seen in the upper portion of the GaP buffer, though contrast near the GaP/Si interface arises due to misfit dislocations. Higher-magnification XTEM comparison showing similarity of 8-period $In_{0.5}Ga_{0.5}As$ SAQDs on (b) epitaxial GaP/Si template and (c) bulk GaP.

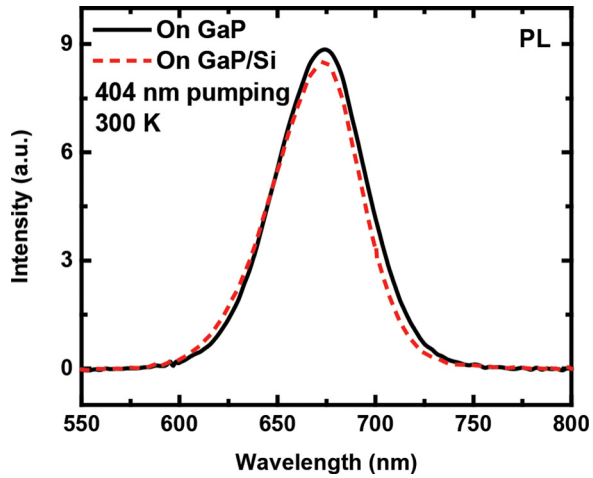

FIG. 3. Room temperature PL spectra of 8-period $In_{0.5}Ga_{0.5}As$ SAQDs on bulk GaP and GaP/Si showing similar integrated intensity, FWHM, and peak wavelength. The close match of the PL spectra on both substrates indicates similar internal quantum efficiency, band structure, and dot size distribution.

that $In_{0.5}Ga_{0.5}As$ SAQDs grown on GaP/Si template are substantially the same as those on bulk GaP.

We then grew and fabricated mesa-isolated LEDs to demonstrate the feasibility of using $In_{0.5}Ga_{0.5}As$/GaP SAQDs as the active region in optoelectronic devices on exact Si (001) substrates. Due to the existence of an epitaxial Si *pn* junction beneath the GaP/Si template, the LEDs fabricated here require two top contacts. Figure 4 shows both the layer structure of the SAQD LEDs and the device structure. The epitaxial structure consists of a 5 μm Si-doped *n*-type bottom current-spreading layer, a 0.1 μm unintentionally doped (UID) active region, a 1 μm Be-doped *p*-type GaP top current-spreading layer, and a 100 nm Be-doped *p*-type GaAs contact layer. The active region contains 8 periods of SAQDs with 3.0 ML of $In_{0.5}Ga_{0.5}As$ per layer. The doping concentrations in the *n*- and *p*-type regions are set to high values of 4.2×10^{18} and $1.0 \times 10^{19}\,cm^{-3}$, respectively, to reduce the sheet resistance in both layers. Although tensile thermal stress in the III-V layers is expected due to thermal mismatch with the Si substrates,[18] no cracking was observed in the devices studied here.

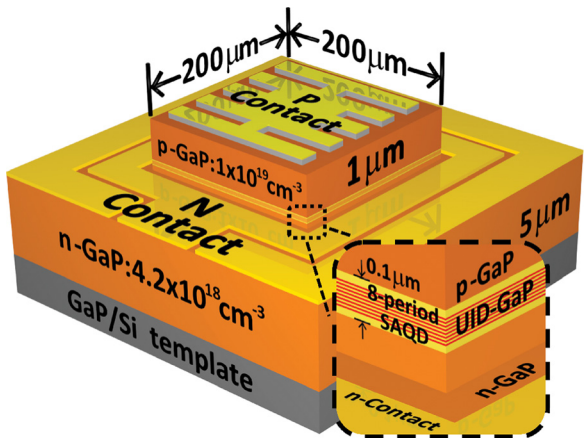

FIG. 4. Layer and device structure of $In_{0.5}Ga_{0.5}As$/GaP SAQD LED on GaP/Si template. Zoomed inset schematically illustrates the 0.1 μm active region, containing 8 periods of SAQDs separated by 10 nm GaP spacers.

The device processing began with lift-off of an e-beam evaporated top-metal stack consisting of 50 Å Cr and 2000 Å Au as the *p*-type contact. Next, a 1.4 μm deep chlorine-based dry etching process defined 200 μm × 200 μm isolated device mesas by etching into the *n*-type GaP regions. Then, 50 Å Ni followed by 2000 Å Au/Ge was evaporated and patterned onto the dry-etched surface as the *n*-type contact. Finally, the top GaAs contact layer was selectively etched using H_2O_2:NH_4OH:H_2O (2:1:50) solution with the Cr/Au serving as a hard mask. The Cr/Au contact on the *p*-type GaAs anode was ohmic as deposited, while a 400 °C 2 min rapid thermal annealing process was necessary to achieve consistent ohmic contacts on the *n*-type GaP cathode.

The $In_{0.5}Ga_{0.5}As$/GaP SAQD LEDs on GaP/Si exhibit typical rectifying current-voltage (I-V) characteristics, reaching a forward current of 10 mA at 1.87 V and a reverse leakage current around −0.1 nA at −2 V [Figure 5(a)]. The ideality factor of 1.73 is typical for wide bandgap diodes where space-charge recombination is dominant at low injection level, e.g., 0.1 nA to 0.1 mA.[23] LEDs were tested using direct current bias, and as expected, the light-output versus current (L-I) characteristic shows a monotonic increase of intensity with driving current [Figure 5(a)]. The EL spectrum in Figure 5(b) shows an emission peak wavelength at ~672 nm (1.85 eV), which is close to the PL peak wavelength from an undoped structure with the same active region [Figure 3]. The interference fringes in the EL spectrum arise from Fabry-Perot interference in the Si/6.1 μm GaP/air cavity;[24] similar fringes are not observed in the PL spectra of Figure 3 due to the much thinner 0.325 μm GaP buffer, which should result in a very large fringe spacing.

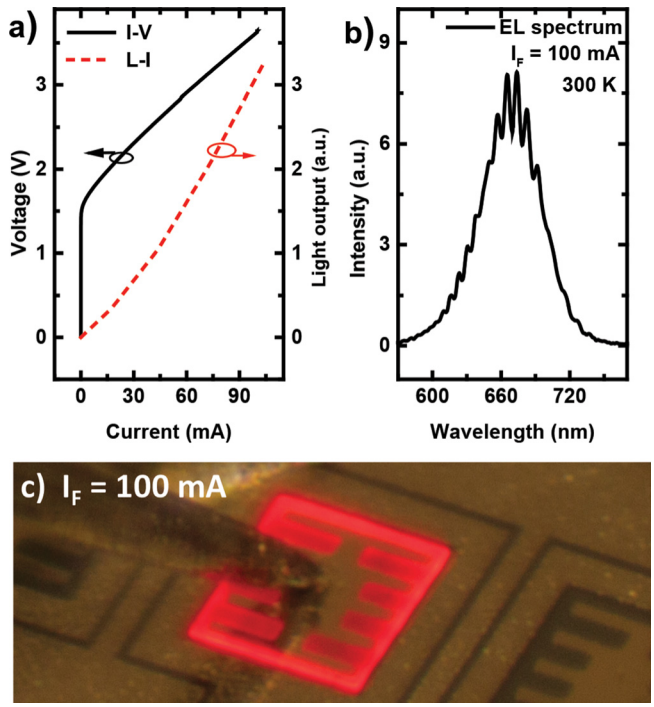

FIG. 5. (a) I-V of SAQD LED on GaP/Si shows typical rectifying characteristics, while L-I shows monotonic increase in light output power with driving current through the testing range. (b) Room temperature EL spectrum of $In_{0.5}Ga_{0.5}As$/GaP SAQD LED on GaP/Si under 100 mA forward current. (c) Micrograph of EL emission from SAQD LED on GaP/Si. All measurements were under direct current bias.

Figure 5(c) shows a photomicrograph of an $In_{0.5}Ga_{0.5}As$/GaP SAQD LED on GaP/Si at 100 mA forward bias. The red EL emission is visible across the LED mesa, though the slightly dark regions between grid fingers indicate insufficient lateral conduction of the top current-spreading layer. In future work, heavy isotype doping in the Si substrate, buffer, and GaP nucleation layer will allow the use of a vertical contact scheme, which will in turn reduce the series resistance (18 Ω in the present work) and remove the necessity for the thick lower current-spreading layer.

In this work, RHEED, XTEM, and PL were used to show nearly identical characteristics of $In_{0.5}Ga_{0.5}As$/GaP SAQDs on both epitaxial GaP/Si (001) templates and GaP (001) substrates. These results prove that growth techniques for $In_{0.5}Ga_{0.5}As$ SAQDs on bulk GaP are readily transferable to GaP/Si templates. Our demonstration of electrically pumped $In_{0.5}Ga_{0.5}As$/GaP SAQD LEDs on exact Si (001) shows that such SAQDs hold great promise for future monolithic integration of optoelectronics with Si-based electronics.

This work was funded by the DARPA Young Faculty Award program (Grant No. N66001-11-1-4148). We are grateful to Dr. B. Kunert ($NASP_{III/V}$ GmbH) for providing GaP/Si template samples and to Dr. J. Lang for AFM measurements. Microscopy facilities used in this work were supported by the Yale Institute for Nanoscience and Quantum Engineering and National Science Foundation MRSEC DMR 1119826.

[1]H. Döscher, T. Hannappel, B. Kunert, A. Beyer, K. Volz, and W. Stolz, Appl. Phys. Lett. **93**, 172110 (2008).
[2]I. Németh, B. Kunert, W. Stolz, and K. Volz, J. Cryst. Growth **310**, 1595 (2008).
[3]T. J. Grassman, M. R. Brenner, S. Rajagopalan, R. Unocic, R. Dehoff, M. Mills, H. Fraser, and S. A. Ringel, Appl. Phys. Lett. **94**, 232106 (2009).
[4]K. Yamane, T. Kobayashi, Y. Furukawa, H. Okada, H. Yonezu, and A. Wakahara, J. Cryst. Growth **311**, 794 (2009).
[5]K. Volz, A. Beyer, W. Witte, J. Ohlmann, I. Németh, B. Kunert, and W. Stolz, J. Cryst. Growth **315**, 37 (2011).
[6]T. J. Grassman, J. A. Carlin, B. Galiana, L.-M. Yang, F. Yang, M. J. Mills, and S. A. Ringel, Appl. Phys. Lett. **102**, 142102 (2013).
[7]S. Liebich, M. Zimprich, A. Beyer, C. Lange, D. J. Franzbach, S. Chatterjee, N. Hossain, S. J. Sweeney, K. Volz, B. Kunert, and W. Stolz, Appl. Phys. Lett. **99**, 071109 (2011).
[8]T. J. Grassman, M. R. Brenner, M. Gonzalez, A. M. Carlin, R. R. Unocic, R. R. Dehoff, M. J. Mills, and S. A. Ringel, IEEE Trans. Electron Devices **57**, 3361 (2010).
[9]J. R. Lang, J. Faucher, S. Tomasulo, K. N. Yaung, and M. L. Lee, Appl. Phys. Lett. **103**, 092102 (2013).
[10]Y. Song, P. J. Simmonds, and M. L. Lee, Appl. Phys. Lett. **97**, 223110 (2010).
[11]T. N. Thanh, C. Robert, C. Cornet, M. Perrin, J. M. Jancu, N. Bertru, J. Even, N. Chevalier, H. Folliot, O. Durand, and A. Le Corre, Appl. Phys. Lett. **99**, 143123 (2011).
[12]G. Stracke, A. Glacki, T. Nowozin, L. Bonato, S. Rodt, C. Prohl, A. Lenz, H. Eisele, A. Schliwa, A. Strittmatter, U. W. Pohl, and D. Bimberg, Appl. Phys. Lett. **101**, 223110 (2012).
[13]C. Prohl, A. Lenz, D. Roy, J. Schuppang, G. Stracke, A. Strittmatter, U. W. Pohl, D. Bimberg, H. Eisele, and M. Dähne, Appl. Phys. Lett. **102**, 123102 (2013).
[14]F. Fukami, K. Umeno, Y. Furukawa, N. Urakami, S. Mitsuyoshi, H. Okada, H. Yonezu, and A. Wakahara, Phys. Status Solidi C **8**, 322 (2011).
[15]C. Robert, C. Cornet, P. Turban, T. N. Thanh, M. O. Nestoklon, J. Even, J. M. Jancu, M. Perrin, H. Folliot, T. Rohel, S. Tricot, A. Balocchi, D. Lagarde, X. Marie, N. Bertru, O. Durand, and A. Le Corre, Phys. Rev. B **86**, 205316 (2012).
[16]K. Rivoire, S. Buckley, Y. Song, M. L. Lee, and J. Vučković, Phys. Rev. B **85**, 045319 (2012).
[17]Y. Song and M. L. Lee, Appl. Phys. Lett. **100**, 251904 (2012).
[18]T. Roesener, V. Klinger, C. Weuffen, D. Lackner, and F. Dimroth, J. Cryst. Growth **368**, 21 (2013).
[19]R. Leon, S. Chaparro, S. R. Johnson, C. Navarro, X. Jin, Y. H. Zhang, J. Siegert, S. Marcinkevičius, X. Z. Liao, and J. Zou, J. Appl. Phys. **91**, 5826 (2002).
[20]H. Tanoto, S. F. Yoon, C. Y. Ngo, W. K. Loke, C. Dohrman, E. A. Fitzgerald, and B. Narayanan, Appl. Phys. Lett. **92**, 213115 (2008).
[21]Y. Fujimoto, H. Yonezu, A. Utsumi, K. Momose, and Y. Furukawa, Appl. Phys. Lett. **79**, 1306 (2001).
[22]N. Sommer, R. Buss, J. Ohlmann, T. Wegele, C. Jurecka, S. Liebich, B. Kunert, W. Stolz, and K. Volz, J. Cryst. Growth **370**, 191 (2013).
[23]S. M. Sze and K. K. Ng, in *Physics Semiconductor Devices* (John Wiley & Sons, Inc., 2006), pp. 96–98.
[24]C. Hums, T. Finger, T. Hempel, J. Christen, A. Dadgar, A. Hoffmann, and A. Krost, J. Appl. Phys. **101**, 033113 (2007).